

Lower and Upper Critical Fields in the Heavy-Electron Superconductor UPt_3

B. S. Shivaram and J. J. Gannon, Jr.

Department of Physics and Engineering Physics, University of Virginia, Charlottesville, Virginia 22901

David G. Hinks

Materials Science Division, Argonne National Laboratory, Argonne, Illinois 60639

(Received 19 May 1989)

We report the first comprehensive measurements of the lower critical field, H_{c1} , for both orientations $H\parallel a$ axis and $H\parallel c$ axis, of the heavy-electron superconductor UPt_3 . An accurate signature for H_{c1} is obtained in a LC oscillator whose resonance frequency changes on flux entry into the superconductor. The H_{c1} values obtained with this technique indicate a "kink" for $H\parallel a$ axis only. With this same technique we also measure the upper critical field, H_{c2} . The results obtained are compared with predictions from recent theories of H_{c1} and H_{c2} in anisotropic superconductors.

PACS numbers: 74.30.Gn, 74.60.Ec, 74.70.Tx

Considerable recent interest has been generated by the observation of two jumps in the specific heat of the heavy-electron superconductor UPt_3 .¹ The origin of the two jumps is suggested to arise from a perturbation that lifts the degeneracy in the transition temperatures of a multicomponent order parameter.²⁻⁴ Another manifestation of this splitting of the phase transition is the "kink" in the upper critical field, H_{c2} , for $H\parallel$ basal plane. This feature suspected in earlier measurements⁵⁻⁷ is well resolved in more recent measurements on purer samples.⁸ Based on this picture, Hess, Tokuyasu, and Sauls have recently predicted that a kink should be observed in the lower critical field, H_{c1} , for all orientations of the field.² Furthermore, it is suggested that the observation of all three features, two jumps in the specific heat, a kink in H_{c2} for $H\parallel$ basal plane, and a kink in H_{c1} for all orientations of the field, in the same set of samples would constitute unambiguous proof for unconventional superconductivity in UPt_3 . The first two features have been observed recently in samples of UPt_3 grown in an ultra-high-vacuum furnace by Taillefer and co-workers.^{8,9} In this Letter we report the observation of the second two features on high-quality single crystals grown with a float-zone-refined technique.¹⁰

Two flat rectangular samples—sample 1 oriented with the c axis in the plane of the sample and sample 2 oriented with the basal plane parallel to the plane of the crystal—were used in the present work. These samples were loosely coupled to the inductance of two separate LC circuits whose resonance frequency could be measured to better than a part in 10^7 . The dimensions of both the samples were $3\times 2\times 0.2$ mm³ and both the external dc field and the rf field in the inductor were parallel to the flat face of the crystals. This geometry ensures that the demagnetizing effects are negligible. The resonant circuit was driven by a tunnel diode and its frequency, f , was measured at constant temperature with the magnetic field H being stepped in small increments.

A change in the resonant frequency of an LC oscillator

can arise by a change in either the inductance or the resistance of the sample coupling to the LC circuit, and is given by the expression¹¹

$$\frac{df}{f} = -\frac{dL}{2L} \left(1 - \frac{2}{Q^2} \right) - \frac{2}{Q^2} \frac{dR}{R}, \quad (1)$$

where L is the total inductance (empty coil plus sample), R is the effective resistance, and Q is the quality factor. For our coils with the sample included at low temperatures the quality factor is about 100. The second term, therefore, can largely be neglected and we are mostly sensitive to inductive changes. A change in the inductance can be introduced by a changing penetration depth in the sample.¹² Another way the inductance of the sample can change is by the nucleation of vortices on the application of an external magnetic field. Thus, sweeping the field at constant temperature should result in a steep decrease in f on flux entry at H_{c1} . As more and more flux lines are created, the inductance continues to increase until H_{c2} at which point the frequency f stops decreasing. Thus, one would expect a change in the slope, df/dH , as a function of magnetic field at H_{c2} . It is possible that this change in slope is further accentuated by the resistance increase at H_{c2} .

In Fig. 1, we show the results we obtained at 0.15 K for both samples, sample 1 with the magnetic field along the c axis and sample 2 with the field along the a axis. For the c -axis experiment the rf magnetic field, h , was oriented perpendicular to the dc field, H , with the plane of the sample being held parallel to both h and H . The upper part of Fig. 1 shows the data obtained for this geometry. There is a sharp change in frequency at low fields where the first vortex is nucleated (we concentrate on this low-field region later—see below), a monotonic decrease in the resonance frequency in higher fields, and a change in slope at the upper critical field. The lower part of Fig. 1 shows the data obtained on sample 2 with the rf field parallel to the external dc field. The low-field

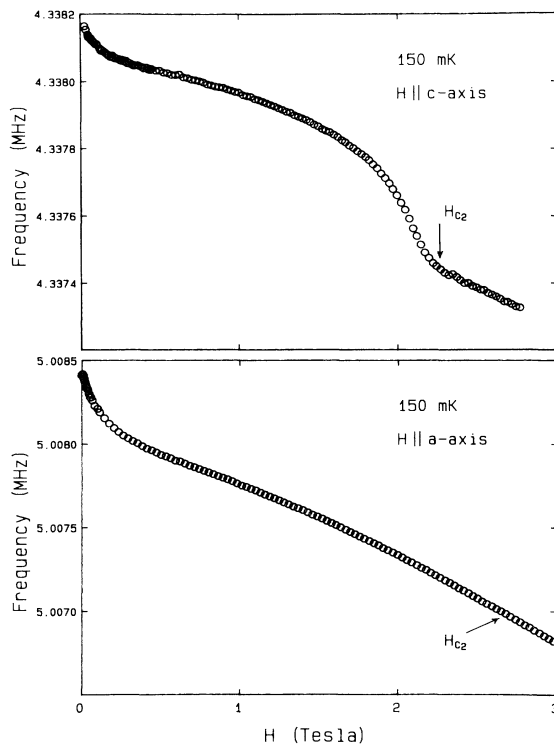


FIG. 1. The resonant frequency of the two circuits with sample 1 and sample 2 (see text) as the magnetic field was stepped in small increments. For the data in the upper part of the figure ($H \parallel c$ axis) the rf coil was oriented perpendicular to the dc magnetic field. In this case there is a clear change in slope at H_{c2} . For $H \parallel a$ axis, however, the ac field was parallel to the dc field. No signature was observed in this geometry near the field where H_{c2} as determined resistively was expected.

behavior is similar to that of sample 1. However, we do not observe any feature for fields near H_{c2} for this geometry. This difference in behavior between the two geometries can be understood by the following arguments.

The rf field applied in these experiments is very small

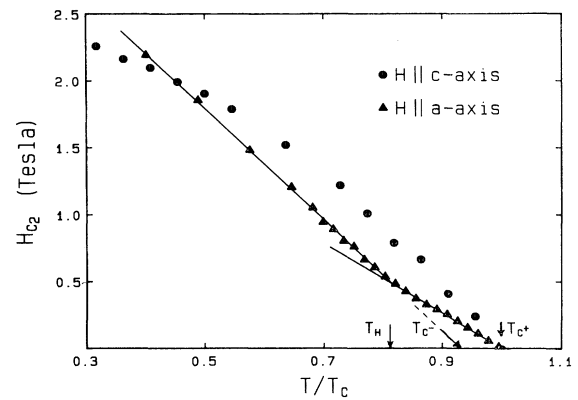


FIG. 2. The upper critical field for both the orientations, $H \parallel c$ axis and $H \parallel a$ axis. The data for $H \parallel c$ axis were obtained by the inductive technique from measurements of the type shown in Fig. 1. For $H \parallel a$ axis, the data were obtained resistively. The lines used to determine the temperatures T_{c+} , T_{c-} , and T_H given in Table I are also shown.

and is approximately 2×10^{-8} T. A field of this magnitude corresponds to about 10 vortices being pushed in and out of the sample at the rf frequency near H_{c2} for the geometry with $h \parallel H$. This is an insignificant fraction to cause either an inductive change or a shift in the resonance frequency due to dissipation in the circuit. On the other hand, a perpendicular rf field creates an oscillation of the entire flux lattice which causes an appreciable dissipation near H_{c2} resulting in an added frequency shift. We also note that for neither of these geometries do we observe any feature in these measurements near $0.6H_{c2}$ corresponding to a possible vortex transition which has been reported recently both in longitudinal-ultrasound¹³ and in torsional-oscillator experiments.¹⁴ The vortex transition is not observed with transverse ultrasound as well.¹⁵ Transverse sound, analogous to the present set of measurements, primarily involves the creation of electromagnet currents without density changes within the sample.

Since sample 2 did not show any feature near H_{c2} we

TABLE I. Parameters obtained from experiment and theory.

		Experiment							
T_{c+} (mK)	T_{c-} (mK)	T_H (mK)	T_{c*} (mK)	$H'_{c1}(-)$ $H'_{c1}(+)$ (c axis)	$H'_{c1}(-)$ $H'_{c1}(+)$ (a axis)	H'_{c2} (T/K) (c axis)	H_{c2} (T/K) (a axis)		
550 ± 10	512 ± 5	448 ± 20	370 ± 40	~ 1.0	3.7 ± 0.5	8.15	4.60		
		Theory							
		$\frac{\beta_2}{\beta_1}$	$\frac{\kappa_1}{\kappa_{123}}$	$H'_{c1}(-)$ $H'_{c1}(+)$ (c axis)	$H'_{c1}(-)$ $H'_{c1}(+)$ (a axis)				
		0.12 ± 0.04	2.3	1.3	1.5				

performed a resistive measurement using an LR-400 resistance bridge as in our earlier work.⁷ In Fig. 2 we show the resistive H_{c2} for $H \parallel a$ axis along with those determined inductively for $H \parallel c$ axis. Several features of this figure are noteworthy. There is a change in the slope dH_{c2}/dT for $H \parallel a$ axis which produces a kink at the temperature T_H . The ratio of the slopes below and above T_H is 1.52. This ratio is somewhat larger than that obtained in earlier experiments.⁷ In Fig. 2 we also identify two other temperatures, T_{c+} and T_{c-} . The experimental values of these various quantities are summarized in Table I.

In Fig. 3 we show the low-field behavior of the measured frequency for both samples. The behavior is characterized by an initial flat response corresponding to the Meissner region of a type-II superconductor and a clear decrease in the resonance frequency beyond a critical field for flux entry into the superconductor. To obtain values for the critical field we performed the following statistical analysis on the data. A tentative value for the lower critical field H_{c1} was identified and a horizontal line fitted to all points at field values less than $0.8H_{c1}$. Next, a linear fit was obtained for all points beyond $1.2H_{c1}$ and the two straight lines were joined smoothly

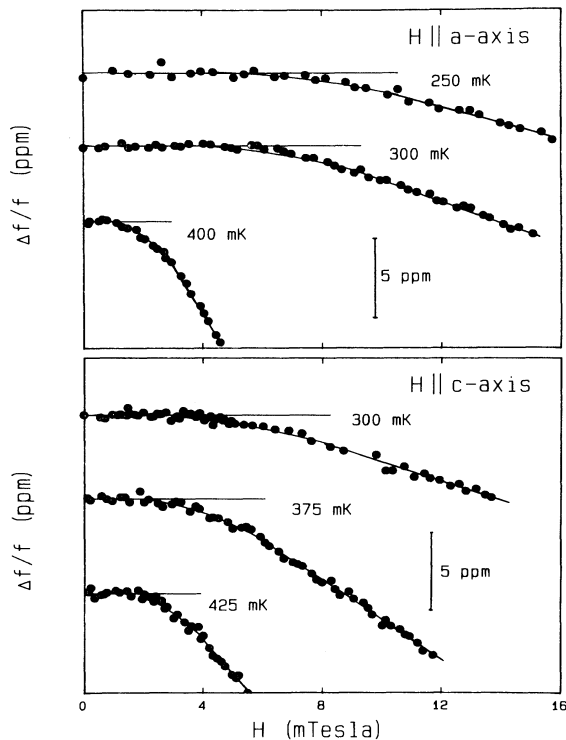


FIG. 3. The low-field behavior for the two orientations at three different temperatures indicated in the figure. H_{c1} is defined as the point of departure of the resonant frequency from the initial horizontal line as the external magnetic field is stepped up.

by a polynomial fit. The final value of H_{c1} was chosen as the point on the fit 3 standard deviations away from the initial horizontal line. The values of H_{c1} obtained this way including the error bars resulting from the statistical fit are shown in Fig. 4. It is clear that our ability to identify the flux-entry field in this technique depends on the extent of deviation of the measured frequency from an initial horizontal line. This deviation was somewhat stronger for sample 2 than for sample 1. As seen in Fig. 4 there is a kink in H_{c1} for $H \parallel a$ axis at the temperature which we label as T_{c*} . For the other orientation, $H \parallel c$ axis, within the limits of our data no such feature is observed.

Using the experimental results presented above we can arrive at a number of fundamental parameters relevant to anisotropic superconductivity in UPt_3 . According to the theory of Hess, Tokuyasu, and Sauls, the two physical transition temperatures, T_{c*} and T_{c+} , and the extrapolated value T_{c-} yield the dimensionless ratio of two

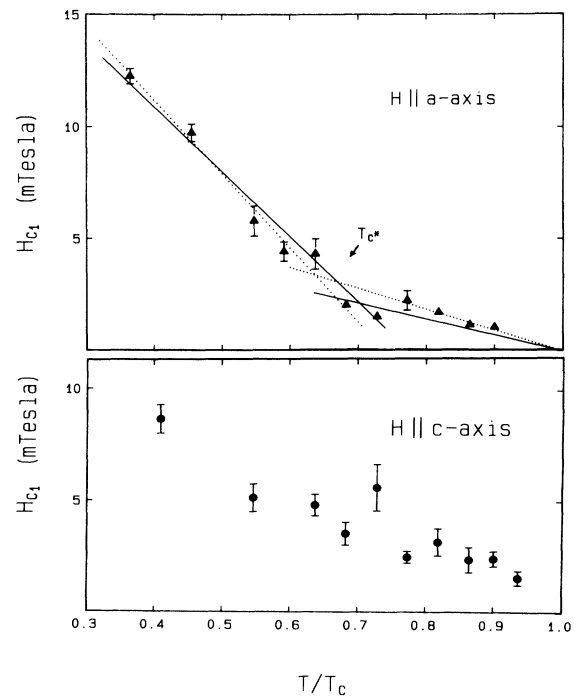


FIG. 4. The lower critical fields for the two orientations determined from the raw data of the type shown in Fig. 3. For $H \parallel a$ axis there is a kink in H_{c1} at the temperature T_{c*} . The solid and the dotted lines represent two of the various possible ways of selecting the points for a two-straight-line fit. The value of T_{c*} mentioned in Table I is the average of these two fits. It is also possible to fit a smooth curve through the experimental points without producing a kink. Such a smoothed behavior would be expected in the presence of spin-orbit and impurity scattering (Ref. 16). We also note that the values for the lower critical field are consistent with dc magnetization measurements in polycrystals of UPt_3 (Ref. 17).

Ginzburg-Landau parameters, β_2/β_1 :

$$T_{c^*} = \frac{T_{c^+} + T_{c^-}}{2} \left\{ 1 - \frac{\beta_1}{\beta_2} \frac{(T_{c^+} - T_{c^-})}{(T_{c^+} + T_{c^-})} \right\}. \quad (2)$$

These parameters also decide the ratio of the heat-capacity jumps at the upper and lower superconducting transitions. Using the experimental values for T_{c^+} , T_{c^*} , and T_{c^-} shown in Table I we find the ratio $\beta_2/\beta_1 = 0.12$. This is in good agreement with estimates for this ratio obtained from the experimental heat-capacity jumps of Fisher *et al.*¹ The other experimentally obtained parameter T_H determines the dimensionless ratio of two other Ginzburg-Landau parameters, κ_1/κ_{123} :

$$T_H = \frac{T_{c^-} - \sqrt{\kappa_1} - T_{c^+} + \sqrt{\kappa_{123}}}{\kappa_1 - \kappa_{123}}. \quad (3)$$

With these two ratios of the Ginzburg-Landau parameters having been determined it is possible to predict the slopes of the lower critical field curves for the a and c axes of the crystal [Eqs. (4) and (5), respectively]:

$$\frac{H'_{c_1}(-)}{H'_{c_1}(+)} = \left(1 + \frac{\beta_2}{\beta_1} \right) \left(\frac{3}{4} + \frac{\kappa_1}{\kappa_{123}} \right), \quad (4)$$

$$\frac{H'_{c_1}(-)}{H'_{c_1}(+)} = \left(1 + \frac{\beta_2}{\beta_1} \right) \left(\frac{\kappa_1}{4\kappa_{123}} + \frac{\kappa_{123}}{4\kappa_1} + \frac{1}{2} \right). \quad (5)$$

The predicted ratio for $H \parallel a$ axis is 1.5 and for $H \parallel c$ axis is 1.3. Experimentally we find a much larger value for the ratio of the slopes below and above T_{c^*} for H along the a axis (see Table I). On the other hand, the smallness of the predicted ratio for H along the c axis could be consistent with the fact that experimentally we are unable to observe any feature.

In conclusion, we have reported a comprehensive set of measurements for H_{c_1} and H_{c_2} in the heavy-electron superconductor UPt₃. Along with a kink in H_{c_2} for $H \parallel a$ axis we also find a kink in H_{c_1} at the second superconducting transition. This is in general agreement with the predictions from recent theories of the double superconducting transition in UPt₃. However, there appear to be quantitative discrepancies. This plus several other

features of H_{c_1} and H_{c_2} in unconventional superconductors are worthy of further experimental investigation.

It is a great pleasure to thank J. Moodera for many useful lessons about the tunnel-diode-oscillator technique and J. Sauls and R. Joynt for many useful conversations. We are also grateful to Daryl Hess for a careful reading of the manuscript. One of us (B.S.S.) acknowledges receipt of an Alfred P. Sloan Foundation Research Fellowship. The work at Argonne National Laboratory was supported by U.S. DOE, Division of Basic Energy Sciences, Contract No. W-31-109-ENG-38, and at the University of Virginia was partially supported by C.I.T. Contract No. MAT-89-002.

¹R. A. Fisher *et al.*, Phys. Rev. Lett. **62**, 1411 (1989).

²D. W. Hess, T. A. Tokuyasu, and J. A. Sauls, J. Phys. Condens. Matter. (to be published).

³R. Joynt, Supercond. Sci. Technol. **1**, 210 (1988).

⁴K. Machida, J. Phys. Soc. Jpn. (to be published).

⁵J. W. Chen *et al.*, Phys. Rev. B **30**, 1583 (1984); F. Piquemal *et al.*, J. Magn. Magn. Mater. **63 & 64**, 469-471 (1987); U. Rauchschwalbe *et al.*, Z. Phys. B **60**, 379 (1985).

⁶K. Scharnberg and R. A. Klemm, Physica (Amsterdam) **135B**, 53 (1985).

⁷B. S. Shivaram, T. F. Rosenbaum, and D. G. Hinks, Phys. Rev. Lett. **57**, 1259 (1986).

⁸L. Taillefer, F. Piquemal, and J. Flouquet, Physica (Amsterdam) **153-155C**, 451 (1988).

⁹K. Hasselbach, L. Taillefer, and J. Flouquet, Phys. Rev. Lett. **63**, 93 (1989).

¹⁰B. S. Shivaram, Y. H. Jeong, T. F. Rosenbaum, and D. G. Hinks, Phys. Rev. Lett. **56**, 1078 (1986).

¹¹J. S. Moodera, R. Meservey, and P. M. Tedrow, IEEE Trans. Magn. **21**, 551 (1985).

¹²B. S. Shivaram, J. J. Gannon, Jr., and D. Hinks (to be published).

¹³A. Schenstrom *et al.*, Phys. Rev. Lett. **62**, 332 (1989); V. Muller *et al.*, Phys. Rev. Lett. **58**, 1224 (1987).

¹⁴R. N. Kleiman, P. L. Gammel, E. Bucher, and D. J. Bishop, Phys. Rev. Lett. **62**, 328 (1989).

¹⁵B. S. Shivaram *et al.*, Phys. Rev. B **35**, 5372 (1987).

¹⁶R. A. Klemm (private communication).

¹⁷A. de Visser, A. Menovsky, and J. J. M. Franse, Physica (Amsterdam) **147B**, 81 (1987).